



PHYSICO-CHEMICAL PROPERTIES AND IN VITRO STABILITY STUDIES OF GREEN SYNTHESIZED GOLD NANOPARTICLES USING PELARGONIUM SIDOIDES

U. M . Badeggi^{1,*}, B. A. Lawal², A. O. Akinfenwa³, Y. O. Ayipo⁴,
Y. Azeh⁵ and M. Z. Dagaci⁶

^{1, 5, 6}, DEPARTMENT OF CHEMISTRY, FACULTY OF APPLIED AND NATURAL SCIENCES, IBRAHIM BADAMASI BABANGIDA UNIVERSITY, LAPAI, PMB 11, NIGER STATE, NIGERIA

^{1, 3}, DEPARTMENT OF CHEMISTRY, CAPE PENINSULA UNIVERSITY OF TECHNOLOGY, BELLVILLE CAMPUS, PO BOX 1906, BELLVILLE 7535, SOUTH AFRICA

², DEPARTMENT OF PHARMACOGNOSY AND DRUG DEVELOPMENT, FACULTY OF PHARMACEUTICAL SCIENCES, UNIVERSITY OF ILORIN, KWARA STATE, NIGERIA

⁴, DEPARTMENT OF CHEMICAL, GEOLOGICAL AND PHYSICAL SCIENCES, KWARA STATE UNIVERSITY, MALETE, KWARA STATE, NIGERIA

E-mail addresses: ¹ umbadeggi@ibbu.edu.ng, ² lawal.ba@unilorin.edu.ng, ³ oa.akeemlaja@gmail.com,
⁴ yusuf.ayipo@kwasu.edu.ng, ⁵ azehy@ibbu.edu.ng, ⁶ dagaci6zago@yahoo.com

ABSTRACT

In the present study, Pelargonium sidoides (PS) extract was used in the green synthesis of AuNPs that was characterized by UV-Vis, TEM, SAED, EDS, XRD, FTIR, and DLS. UV-Vis showed a surface plasmon resonance (SPR) at λ_{max} of 532 nm while TEM shows that the particles are predominantly spherical and monodispersed. DLS measurement indicated the particle size and the zeta potential to be 27.20 nm and -24.0 mV respectively. The in vitro stability of the hybrid particles in different solutions and buffers (pH 7 and 9) confirmed that the particles are stable over a given period. The method employed is simple, environmentally friendly, and inexpensive. Our studies suggest that the Pelargonium sidoides-gold nanoparticles (PS-AuNPs) may be safely used in biomedical applications such as drug delivery.

Keywords: *Pelargonium sidoides; biosynthesis; biomedical; capping agent; zeta potential*

1. INTRODUCTION

Nowadays, gold nanoparticles (AuNPs) have found interesting biomedical applications such as in drug delivery, cancer treatment, photothermal and photodynamic therapy [1]. This is due to their interesting physical characteristics such as surface plasmon resonance which can be used for a variety of applications by tuning the size, shape, and morphology [2-3]. To produce AuNPs, physical and chemical methods were popular until sophisticated instrumentation, cost of analysis [4] and the hazardous chemicals employed became a concern, especially when the nanoparticles (NPs) are targeted for biomedical applications [5].

Consequently, the green synthesis methods which applies the principles of green chemistry became better alternatives. Here, harsh chemicals are totally avoided [6]. Among the biological resources, plants are the most abundant, readily available, non-toxic, inexpensive, and the chemicals employed are usually environmentally friendly [7]. Plants are rich sources of phytochemicals that possess reducing as well as capping abilities [3]. Recently, renewed attention has been given to the Metal Nanoparticles (MNPs) like gold and silver because of many unique features of these materials [7-8]. Thus, AuNPs with interesting biological applications have been synthesized using aqueous solutions of *Leucosidea sericea*, *Hypoxis*

* Corresponding author, tel: +27 – 658 – 586 – 907

hemerocallidea, *Galenia Africana*, *Chamaecostus cuspidatus*, *escin*, waste fruits, and citrus extracts [2, 4, 6, 9–11]. Apart from whole plants, extracts of different parts of plants such as flowers, leaves and seeds, leaves, stem bark, and roots [8, 12, 13] have been employed in the green synthesis of MNPs with promising biological activities. On the other hand, *Pelargonium sidoides* (PS) is an important medicinal plant that is native to Southern Africa. Among other parts of PS, the roots have been extensively used in the treatment of ailments such as common cold and cough, dysmenorrhea, gastrointestinal and respiratory disorders, hepatic disorders and diarrhea [14]. These claims were validated by modern research results whereby the roots of PS showed potent antiviral, antifungal, antibacterial [15], antioxidant [16], and antimicrobial [17] properties. Phytochemical screening of the roots revealed that it contained polyphenols, terpenoids, proanthocyanins, and flavonoids [18-19]. These phytoconstituents may serve as reducing and/or stabilizing agents in the synthesis of NPs. Therefore, in the present study, the lyophilized PS root was used in the biosynthesis of gold nanoparticles. The particles were characterized using different microscopic analyses, and the *in vitro* stability was examined. To the best of our knowledge, this is the first report on the synthesis, characterization, and *in vitro* stability evaluation of AuNPs using PS root extract.

2. MATERIALS AND METHODS

2.1 Materials

Dried *Pelargonium sidoides* roots were purchased from local herb seller in Bellville, South Africa. Polystyrene 96-well microtitre plates were obtained from Greiner bio-one GmbH (Frickenhausen, Germany). Sodium tetrachloroaurate (III) dihydrate and Sodium Chloride (NaCl) were procured from Sigma-Aldrich (Cape Town, South Africa). N-Acetyl-L-cysteine (CYS), glycine (GLY), and Phosphate buffered saline (PBS) were purchased from Lonza (Cape Town, South Africa). Bovine serum albumin (BSA) was purchased from Miles Laboratories (Pittsburgh, PA, USA). Deionized water was used throughout.

2.2 Preparation of P. sodoides

The dried plant material was chopped into smaller pieces and further blended affording the powdered form. To obtain the aqueous extract, 10.0 g of the dried material was added to 100.0 mL of boiled

deionized water [11]. After cooling, the decoction was centrifuged for 1 h at 4000 rpm using an Allegra® X-12R centrifuge (Beckman Coulter, Cape Town, South Africa). Then, the supernatant was filtered through 0.45 µm filters and freeze-dried using Free Zone 2.5 L freeze-dryer (Labconco, Kansas City, MO, USA).

2.3 Synthesis of the PS-AuNPs and their Characterization

2.3.1 Synthesis of PS-AuNPs

The freeze-dried material (0.04 g) was dissolved in 2 mL deionized water. 1 mL of the solution was added to 50 mL of gold salt solution (1.0 % wt) that has been heated to about 90 °C on a magnetic stirrer. Within 1 min, a color change from brown to ruby red was observed. The heat was removed and the stirring was continued for another 10 minutes and then allowed to cool to room temperature before UV-Vis and DLS measurements were taken [7].

2.3.2 Characterization of PS-AuNPs

UV-VIS spectroscopy analyses were performed with a Nicolette Evolution 100 Spectrometer (Thermo Electron, UK) to determine the optical properties. The zeta potential and hydrodynamic size values of the PS-AuNPs were measured using a Zetasizer (Malvern Instruments Ltd., Malvern, UK) at 25 °C and a 90° angle. The FTIR analysis was done using the Perkin Elmer spectrophotometer (Waltham, MA, USA). The HRTEM images were obtained using FEI Tecnai G2 20 field-emission gun (FEG) HRTEM operated in bright field mode at an accelerating voltage of 200 kV. The elemental composition of the AuNPs was identified using EDX liquid nitrogen cooled Lithium doped Silicon detector. The crystalline structures of the sample were determined by X-ray diffraction (XRD; X-ray diffraction Model Bruker AXS D8 advance) with radiation at $\lambda_{CuK\alpha 1} = 1.5406 \text{ \AA}$. The image analysis software ImageJ 1.50b version 1.8.0_60 (<http://imagej.nih.gov/ij>) and Origin pro 2019 64 bits were used to analyze the TEM and XRD images.

2.3.4 Stability Evaluation of PS-AuNPs

To measure the effect of different media (e.g., 1% NaCl, 0.5% CYS, GLY, and BSA) on the stability of the biosynthesized AuNPs, 200 µL of the AuNPs solutions were mixed with 100 µL of the buffer solutions or media in a 96-well microtitre plate. The stability of the AuNPs was monitored by measuring the UV-Vis spectrum (between 450 and 700 nm) of the samples at 0, 12, 24, and 48 hrs [11].

3. RESULTS AND DISCUSSION

3.1 UV-Visible spectroscopy of PS-AuNPs

UV-Visible spectroscopy is a technique that is widely used to measure the absorption of nanomaterials. Because different nanomaterials have distinct absorption peaks, the technique is used to confirm the formation of nanoparticles. Figure 1 shows the typical UV-Vis spectrum of PS-AuNPs. A strong absorption can be observed at 532 nm which is the characteristic region for gold nanoparticles. This type of absorption is also known as surface plasmon resonance (SPR). The SPR originates from the oscillation of the conduction of electrons as it interacts with electromagnetic radiation. Similar SPR for gold nanoparticles has been reported previously [2, 11]. The fact that the absorption is sharp and narrow affirmed the successful fabrication of monodispersed PS-AuNPs

3.2 X-ray Diffraction (XRD) and selected area electron diffraction (SAED) Analysis

Figure 2A shows the XRD pattern of PS-AuNPs. The XRD analysis of the as-synthesized PS-AuNPs were carried out to examine the crystallinity of the particles. PS-AuNPs displayed five distinct diffraction peaks in the 2θ range of 30° – 90° that was indexed to the planes (111), (200), (220), (311), and (222) of the face-centred cubic (FCC) gold particles. These peaks were positioned at 38.2° , 44.4° , 64.6° , 77.5° , and 81.7° (Figure 2A). The XRD analysis showed

predominant peaks at (111) indicating the presence of crystallite particles [10]. This fact was further corroborated by the bright rings displayed by SAED (Figure 2B).

3.3 Transmission Electron Microscopy (TEM) and Energy Dispersive X-Ray Spectroscopy (EDS) Analysis

The TEM results, histogram from particle count, and the EDS of PS-AuNPs was displayed in figure 3. The average particle diameter as calculated from 3A indicated that the majority of the seeds are in the 15 nm size, mostly spherical. It also depicts well-dispersed particles. Few triangles and hexagons were however observed as clearly shown in Figure 3B.

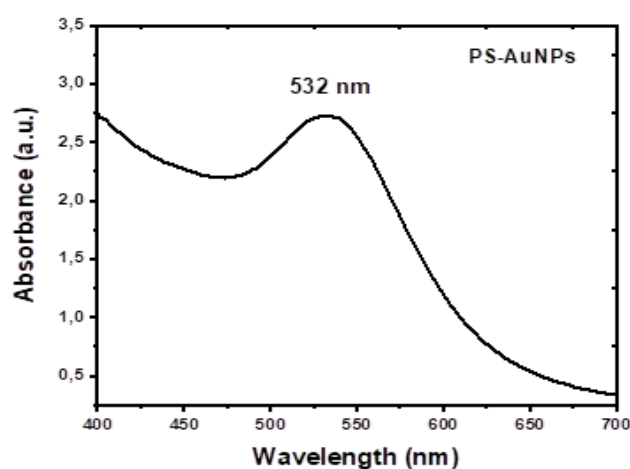


Figure 1: UV-Vis spectra of the biosynthesized PS-AuNPs

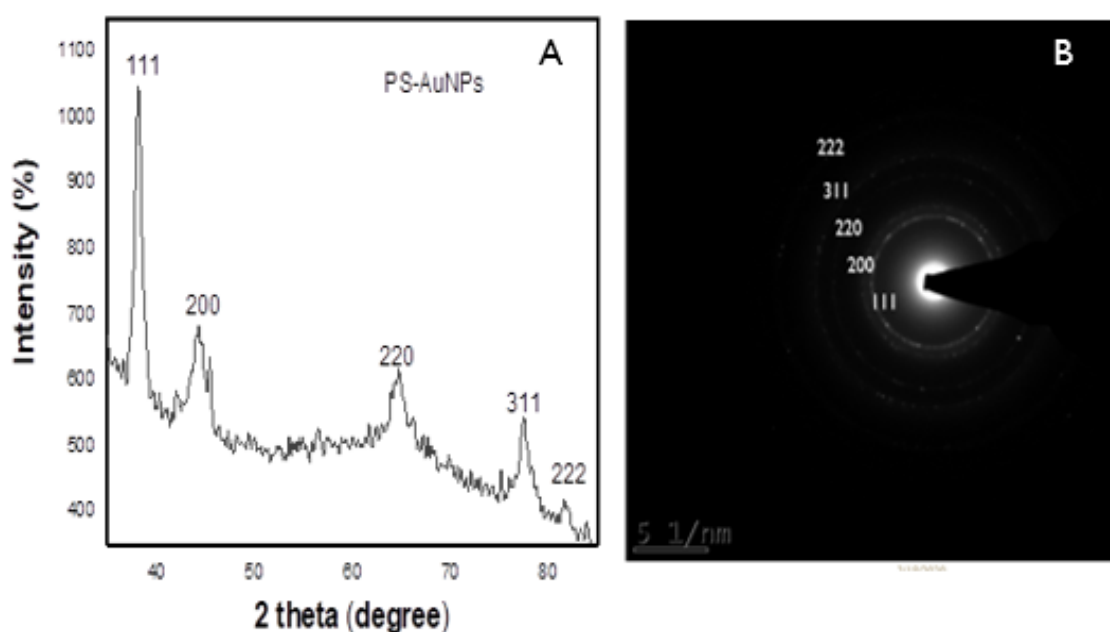


Figure 2: XRD patterns (A) and SAED (B) of PS-AuNPs

This is a characteristic of gold nanoparticles from plant extracts which further validates the successful fabrication of the gold nanoparticles. Another evidence of the formation is the elemental composition analysis (Figure 3D). Clusters of gold atoms were observed in the spectrum at about 9-11 keV. This confirms that the nanomaterial we synthesized is that of gold. Similar TEM and EDS for AuNPs has been reported previously [11].

3.4 FTIR Spectra of PS-AuNPs

Figure 4 represents the FTIR spectra of PS extract and PS-AuNPs. The strong band at $3,204\text{ cm}^{-1}$ corresponded to the O-H stretch vibration of phenols and alcohols which was shifted to $3,222\text{ cm}^{-1}$ in PS-AuNPs. Similarly, the band at $1,609\text{ cm}^{-1}$ that was initially assignable to PS became $1,605\text{ cm}^{-1}$ for PS-AuNPs. This can be ascribed to -C=C- stretching of

carbonyl amide I. Proteins, peptides or amino acid groups are usually thought to be involved in the reduction and stabilizing process when this band is identified in AuNPs. The peaks at $1,346\text{ cm}^{-1}$ and $1,338\text{ cm}^{-1}$ in both PS extracts and PS-AuNPs corresponded to the O-H bending of phenols. This further confirms the O-H stretch earlier mentioned. Interestingly, a new peak appears at 1203 cm^{-1} which was not observed in PS. Therefore, in addition to the change from 1040 to 1033 cm^{-1} , the peaks are assignable to the C-O stretching of alkyl aryl ether. The presence of these functional groups confirmed other researchers claim that the root of PS may contain proanthocyanins, polyphenols, terpenoids, and flavonoids [18-19] and they might be involved in the bioreduction and subsequent stabilization of PS-AuNPs.

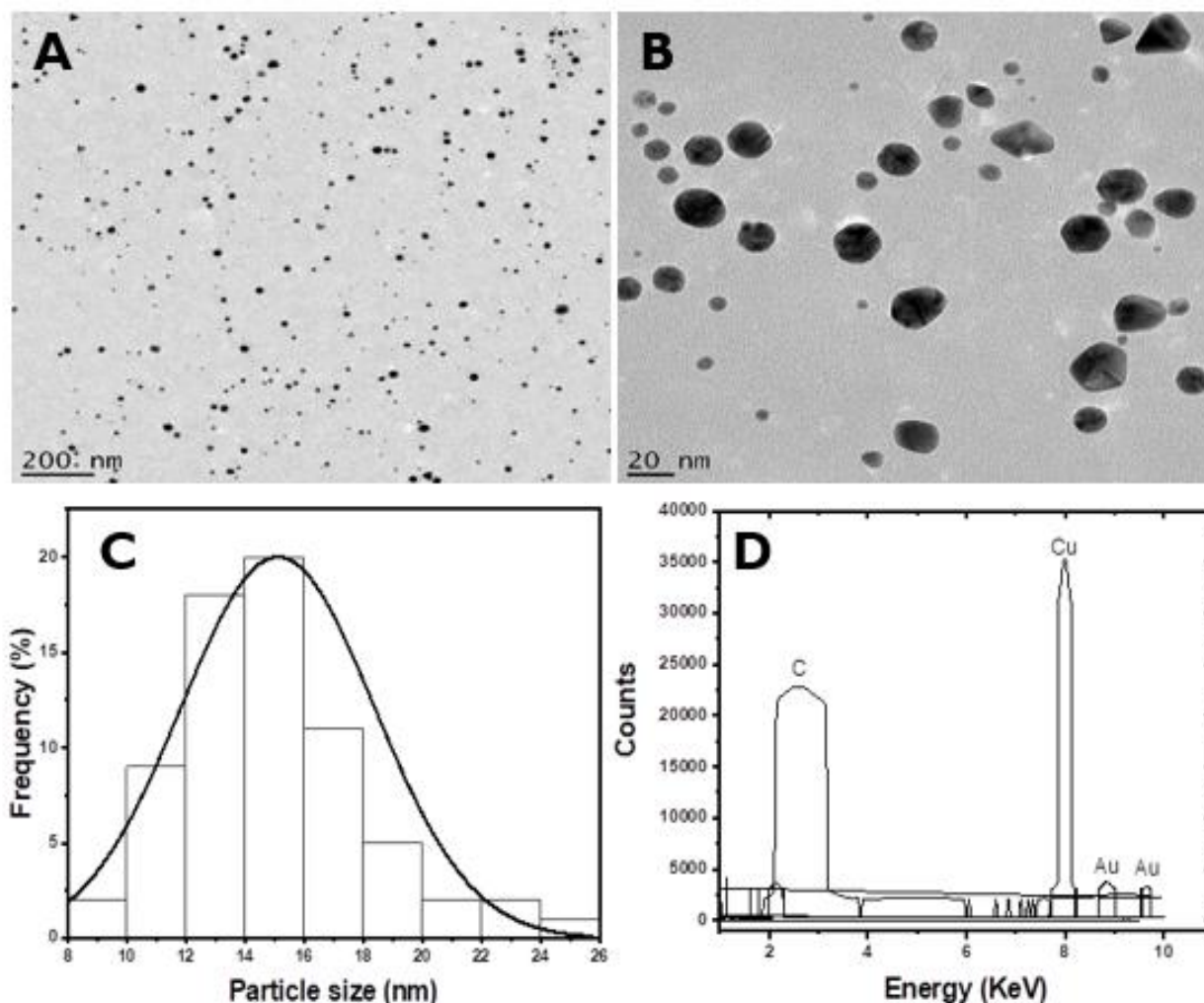


Figure 3: TEM images (A, B), histogram (C) and EDS (D) of PS-AuNPs

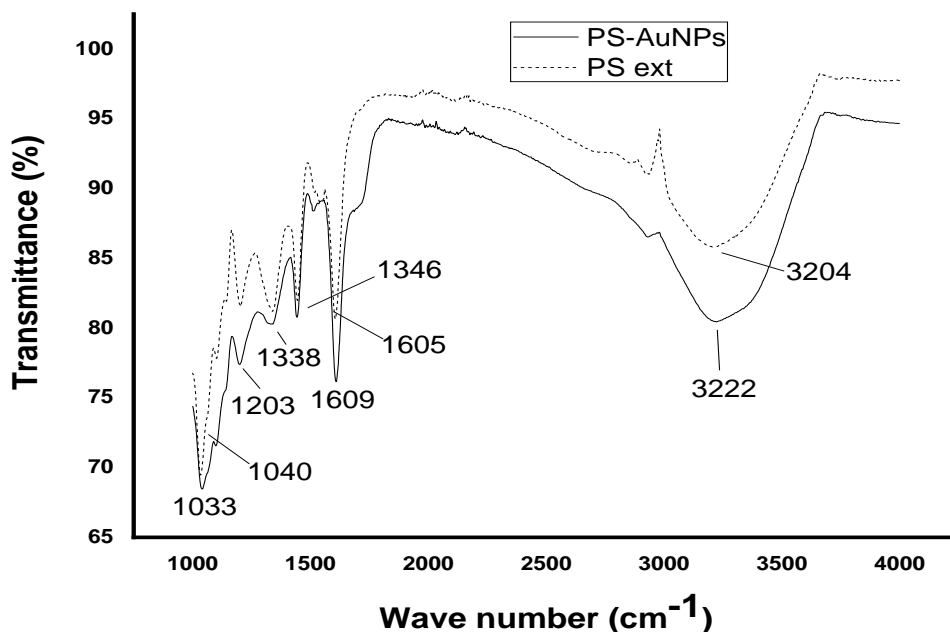


Figure 4: FTIR spectrum of PS and PS-AuNPs

3.5 Dynamic Light Scattering (DLS) measurement of PS-AuNPs

DLS is a well-established technique that is used to measure the hydrodynamic size and surface charge of nanomaterials. The average size of PS-AuNPs was 27.20 nm whereas the zeta potential was -24.0 mV. Zeta potential (ZP) is related to the surface charge of nanoparticles and so particles with ZP less than -30 mV are considered strongly anionic [7]. The polydispersity index (PDI) of our AuNPs was 0.261, a low index which is an indication of high homogeneity of the particles. The zeta potential value of -24.0 mV (Table 1) shows that large negative ions existed on the surface of our particles. It further implies that a strong repulsive force is present in the assembly of ions thereby enhancing stability. The higher the negative value of ZP, the better the stability. Accordingly, highly stable particles have fewer chances of aggregation and this is a crucial requirement for the particles to maintain their properties [14]. This will then qualify them for biomedical applications.

3.7 *In vitro* stability evaluation

Since the potential application of the synthesized PS-AuNPs is biomedical, the *in vitro* stability of PS-AuNPs was evaluated using 0.5% BSA, GLY, CYS, 1% NaCl,

and buffers (pH 7 and 9) as shown in Figure 6. These were studied alongside the undiluted particles and the absorbance was monitored by UV-Vis spectrophotometer. First Reading was immediately the media and buffer were added (0 hr) in a 96-well plate. The second was after 12 hrs incubation at room temperature (12 hrs), the third and fourth measurements were taken after 24 and 48 hrs incubation respectively at 37°C. The spectral studies showed that PS mediated gold nanoparticles are intact for these periods. Between 0 and 12 hrs, there was hardly any blue or red shift. The surface plasmon resonance in all the physiological medium remained about the same regions except for a shift from the particle by approximately 0.5 nm at 48 hrs. Overall, these slight shifts are considered acceptable and therefore the nanoparticles are stable at all the physiological solutions tested. Furthermore, it can be observed that the biological solutions were selected to mimic the conditions in the human system to get the picture of the behavior of our particles when the study would be graduated into the *in vivo* stage. By this, pH 7 would have been enough but we went further to pH 9 for additional information. From Figure 6, it is evident that even at such high pH value, the particles were still properly dispersed, avoiding agglomeration.

Table 1: Particle size and zeta potential of PS-AuNPs

Sample	Hydrodynamic size (nm)	Zeta potential (mV)	Polydispersity index
PS-AuNPs	27.20	-24.0	0.261

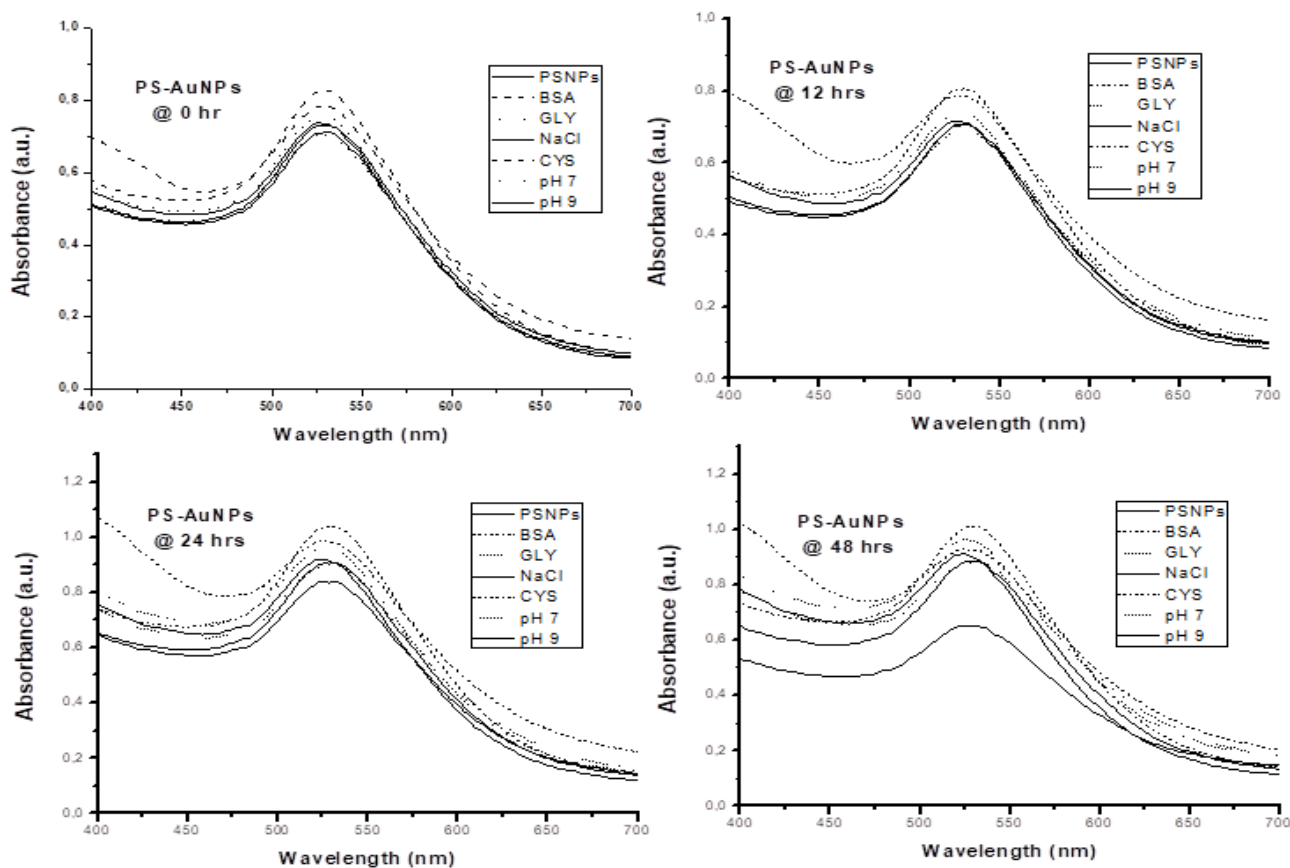


Figure 6: *In vitro* stability measurements by UV-Vis at different time interval

This further confirms the results of zeta potential, thereby validating the suitability of our hybrid particles for biomedical applications.

4. CONCLUSION

The aqueous extract of freeze-dried PS root was used to synthesize PS-AuNPs through a green route for the first time. PS-AuNPs were characterized and displayed high stability by DLS measurement and at physiological conditions *in vitro*. Thus, the method is simple, fast, inexpensive, eco-friendly, and validates the potential biomedical applications of the biocompatible nanomaterial synthesized in this study.

5. ACKNOWLEDGMENTS

We would like to thank Prof Ahmed Mohammed of CPUT, South Africa for using the facilities in his research laboratory and Dr. Subelia Botha of UWC, South Africa for TEM, EDS and SAED analysis.

6. CONFLICTS OF INTEREST

The authors declare no conflicts of interest.

7. REFERENCES

- [1] R. Vankayala, C. L. Kuo, A. Sagadevan, P. H. Chen, C. S. Chiang, and K. C. Hwang, 'Morphology dependent photosensitization and formation of singlet oxygen ($^1\Delta_g$) by gold and silver nanoparticles and its application in cancer treatment', *Journal of Materials Chemistry B*, Vol. 1, Number 35, 2013, pp. 4379–4387.
- [2] B. R. Shamprasad, S. Keerthana, S. Megarajan, R. Lotha, S. Aravind, and A. Veerappan, 'Photosynthesized escin stabilized gold nanoparticles exhibit antidiabetic activity in L6 rat skeletal muscle cells', *Materials Letters*, Vol. 241, 2019, pp. 198–201.
- [3] M. Ovais, A. T. Khalil, N. U. Islam, I. Ahmad, M. Ayaz, M. Saravanan, Z. K. Shinwari, and S. Mukherjee, 'Role of plant phytochemicals and microbial enzymes in biosynthesis of metallic nanoparticles', *Applied Microbiology and Biotechnology*, Vol. 102, Number 16, 2018, pp. 6799–6814.
- [4] K. Mohan Kumar, B. K. Mandal, M. Sinha, and V. Krishnakumar, 'Terminalia chebula mediated green and rapid synthesis of gold nanoparticles', *Spectrochim. Acta - Part A Molecular and Biomolecular Spectroscopy*, Vol. 86, 2012, pp. 490–494.
- [5] A. M. Fayaz, M. Girilal, S. A. Mahdy, S. S. Somsundar, R. Venkatesan, and P. T.

- Kalaichelvan, 'Vancomycin bound biogenic gold nanoparticles: A different perspective for development of anti VRSA agents', *Process Biochemistry*, Vol. 46, Number 3, 2011, pp. 636–641.
- [6] J. Yu, D. Xu, H. Nan, C. Wang, L. Kun, and D. F. Chi, 'Facile one-step green synthesis of gold nanoparticles using Citrus maxima aqueous extracts and its catalytic activity', *Materials Letters*, Vol. 166, Number 26, 2016, pp. 110–112.
- [7] U. M. Badeggi, E. Ismail, A. O. Adeloje, S. Botha, J. A. Badmus, J. L. Marnewick, C. N. Cupido and A. A. Hussein, 'Green Synthesis of Gold Nanoparticles Capped with Procyanidins from Leucosidea sericea as Potential Antidiabetic and Antioxidant Agents', *Biomolecules*, Vol. 10, Number 3, 2020, pp. 452.
- [8] M. Shah, S. Nawaz, H. Jan, N. Uddin, A. Ali, S. Anjum, N. Giglioli-Guivarc'h, C. Hano, and B.H. Abbasi, 'Synthesis of bio-mediated silver nanoparticles from Silybum marianum and their biological and clinical activities', *Materials Science and Engineering: C*, Vol. 112, 2020, pp. 110889.
- [9] M. Ponnaniakamdeen and S. Rajeshkumar, 'In Vivo Type 2 Diabetes and Wound-Healing Effects of Antioxidant Gold Nanoparticles Synthesized Using the Insulin Plant Chamaecostus cuspidatus in Albino Rats', *Canadian Journal of Diabetes*, Vol. 43, Number 2, 2019, pp. 82-89.
- [10] J. K. Patra and K. H. Baek, 'Comparative study of proteasome inhibitory, synergistic antibacterial, synergistic anticandidal, and antioxidant activities of gold nanoparticles biosynthesized using fruit waste materials', *International Journal of Nanomedicine*, Vol. 11, 2016, pp. 4691–4705.
- [11] A. M. Elbagory, M. Meyer, C. N. Cupido, and A. A. Hussein, 'Inhibition of Bacteria Associated with Wound Infection by Biocompatible Green Synthesized Gold Nanoparticles from South African Plant Extracts', *Nanomaterials*, Vol. 7, Number 12, 2017, pp. 417.
- [12] S. Valsalam, P. Agastian, M.V. Arasu, N.A. Al-Dhabi, A.K.M. Ghilan, K. Kaviyarasu, B. Ravindran, S.W. Chang, and S. Arokiyaraj, 'Journal of Photochemistry & Photobiology, B: Biology Rapid biosynthesis and characterization of silver nanoparticles from the leaf extract of Tropaeolum majus L. and its enhanced in-vitro antibacterial, antifungal, antioxidant and anticancer property', *Journal of Photochemistry and Photobiology B: Biology*, Vol. 191, 2019, pp. 65–74.
- [13] I. R. Beattie and R. G. Haverkamp, 'Silver and gold nanoparticles in plants: Sites for the reduction to metal', *Metallomics*, Vol. 3, Number 6, 2011, pp. 628–632.
- [14] S. M. Park, B.G. Min, J. Y. Jung, K. H. Jegal, C. W. Lee, K. Y. Kim, Y. W. Kim, Y. W. Choi, I. J. Cho, S. K. Ku, and S. C. Kim, 'Combination of Pelargonium sidoides and Coptis chinensis root inhibits nuclear factor kappa B-mediated inflammatory response in vitro and in vivo', *BMC Complementary and Alternative Medicine*, Vol. 18, Number 20, 2018, pp. 1–13.
- [15] S. Samie, K. M. Trollope, L. Joubert, and N. P. Makunga, 'The antifungal and Cryptococcus neoformans virulence attenuating activity of Pelargonium sidoides extracts', *Journal of Ethnopharmacology*, Vol. 235, Number 10, 2019, pp. 122-132.
- [16] V. Unsal, E. B. Kuruta, M. Gungor, A. M. Emrah, 'Role of protective Pelargonium Sidoides root extract and Curcumin on Role of protective Pelargonium sidoides root extract and curcumin on mushroom ushroom poisoning; An experimental xperimental study in rats', *International Journal of Phytomedicine*, Vol. 9, Number 2, 2017, pp. 261-266.
- [17] Z. Aboobaker, A. Viljoen, W. Chen, P. W. Crous, V. J. Maharaj, and S. Van Vuuren, 'South African Journal of Botany Endophytic fungi isolated from Pelargonium sidoides DC: Antimicrobial interaction and isolation of a bioactive compound', *South African Journal of Botany*, Vol. 122, 2019, pp. 535–542.
- [18] N. Savickiene, A. Jekabsone, L. Raudone, A. S. Abdelgeliel, A. Cochis, L. Rimondini, E. Makarova, S. Grinberga, O. Pugovics, M. Dambrova, and I. M. Pacauskiene, 'Efficacy of Proanthocyanidins from Pelargonium sidoides Root Extract in Reducing P. gingivalis Viability While Preserving Oral', *Materials*, Vol. 11, Number 9, 2018, pp. 1499.
- [19] M. A. Bisi-johnson, C. L. Obi, B. B. Samuel, J. N. Eloff, and A. I. Okoh, 'Antibacterial activity of crude extracts of some South African medicinal plants against multidrug resistant etiological agents of diarrhoea', *BMC Complementary and Alternative Medicine*, Vol. 17, Number 321, 2017, pp. 1–9.